Distribution pattern of invasion-related bio-markers in head Marjolin's ulcer

ZHIHUI NI[1,2], ZHAO ZHENG[1,2], ENXING YU[1,2], CAN ZU[1,2], DONGDONG HUANG[1,2], KE WU[1,2], JIANGNAN HU[3], SHENG YE[1,2], QICHUAN ZHUGE[1,2], JIANJING YANG[1,2] and LINHUI RUAN[1,2]

[1]Zhejiang Provincial Key Laboratory of Aging and Neurological Disorder Research; [2]Department of Neurosurgery, The First Affiliated Hospital of Wenzhou Medical University, Wenzhou, Zhejiang 325000, P.R. China; [3]Department of Pharmaceutical Sciences, University of North Texas Health Science Center, Fort Worth, TX 76107, USA

Received July 24, 2019; Accepted January 14, 2020

DOI: 10.3892/etm.2020.9034

Abstract. Marjolin's ulcer (MU) is a rare and aggressive cutaneous malignancy that typically presented in an area of traumatized or chronically inflamed skin and particularly in burn scars. Among them, the MU in the scalp with extensive invasion of the skull is exceptional and severe. The principle of management for MU is to obtain an early diagnosis and perform prompt surgical interventions. The invasive capacity of MU may vary among different sites of the scalp, which may require different therapeutic strategies for surgical excision. However, no clear evidence has been provided to determine the invasion ability of MU at different regions of the lesion as a surgical guidance. In present study, a 41-year-old female with a 40-year history of scalp ulceration has been examined. After resection of the MU lesion, hematoxylin and eosin (H&E) staining was performed to confirm the pathology of the cutaneous malignancy after surgical excision. Furthermore, reverse transcription-quantitative PCR experiment was performed out to determine the expression levels of invasion-associated biomarkers at different sites of the scalp affected by MU. Pathological analysis with H&E staining indicated a differentiated squamous cell carcinoma with invasion of the skull. The invasion-associated biomarkers were highly expressed in the core region compared to the middle region as well as the edge of MU tissue. Taken together, the present study suggests that the expression pattern of invasion-associated biomarkers varies between different regions of the MU lesion. High expression levels in the core region of MU indicates that the resection of the center area may be critical for the successful surgical treatment of MU.

Correspondence to: Dr Jianjing Yang, Zhejiang Provincial Key Laboratory of Aging and Neurological Disorder Research, The First Affiliated Hospital of Wenzhou Medical University, 8 Fanhaixi Road, Wenzhou, Zhejiang 325000, P.R. China
E-mail: yangjianjing2@yeah.net

Dr Linhui Ruan, Department of Neurosurgery, The First Affiliated Hospital of Wenzhou Medical University, 8 Fanhaixi Road, Wenzhou, Zhejiang 325000, P.R. China
E-mail: ruanlh522@163.com

Abbreviations: MU, Marjolin's ulcer; RT-qPCR, reverse transcription-quantitative PCR; SCC, squamous cell carcinoma; TME, tumor microenvironment; EMT, epithelial-mesenchymal transition; ECM, extracellular matrix; MMPs, matrix metalloproteinases; cDNA, complementary DNA; DSG, desmoglein

Key words: head Marjolin's ulcer, tumor invasion, tumor microenvironment, cell adhesion, cell signaling pathways

Introduction

Marjolin's ulcer (MU) is a rare and aggressive cutaneous malignancy that typically develops in an area of traumatized or chronically inflamed skin, particularly in burn scars (1,2). The incidence of burn scars undergoing malignant transformation is approximately 0.77% ~ 2% (3). Squamous cell carcinoma (SCC) is the most common pathologic type of MU (4). However, compared to conventional skin SCC, MU tends to be more aggressive. In 1828, Marjolin reported a case of malignant ulcer secondary to burn scar and the term 'Marjolin's ulcer' has then been applied to describe malignant tumors occurring in post-traumatic scars (5). MU usually occurs on the extremities, the joints, or other regions of the body that have a high level of mobility, and MU on the head has been rarely reported. Lesions of MU on the head are mainly include burn scar carcinomas of the scalp and are capable of skull bone destruction (6). When MU cells invade the skull, affected patients have a higher risk of higher morbidity rate and a worse outcome (7). In order to suppress invasion of the skull and potentially the brain tissue, expeditious and wide excision of MU lesions at early time-point is necessary and should be the principle of surgical treatment. Furthermore, elucidation of the invasion ability in different regions of the tumor may help develop a proper strategy for surgical resection and comprehensive management. In solid epithelial cancer, the invasion ability of tumor cells is a crucial requirement for cancer progression, which appears to be the most complex and least understood process. Previous studies have indicated that numerous have showed that many factors and signaling pathways are involved in the dynamic invasion process of cancer cells (8). The

important initial step is the separation of tumor cells from the adjacent stroma to progress to the early stages of cancer formation (9). Due to the reduction of cell-to-cell adhesion and acquisition of invasive capabilities by epithelial-mesenchymal transition (EMT), tumor cells may transmigrate through the basement membrane (10). During the EMT process, cancer cells may become even more separated from each other due to the abnormal regulation of cell adhesion molecules (e.g., E-cadherin, claudin, and desmoglein). Furthermore, EMT allows tumor cells to undergo multiple biochemical transformations which strengthen their ability to invade and migrate, as well as marked increases in the production of extracellular matrix matrices (ECM) components. This creates a favorable tumor microenvironment (TME) for the surrounding cancer cells (11). More specifically, TME has a vital role in tumorigenesis and particularly in tumor invasion. Certain molecules in TME, including matrix metalloproteinase (MMP)-2, MMP-9, MMP-14 and periostin) promote the invasiveness of cancer cells. In addition, errors occurring in the cell signaling interactions and cellular information processing may also be responsible for the diseases including such as cancer, as cell signaling is a part of any communication process which governs basic activities of cells and coordinates all cell actions (8). For instance, the receptor activator of NFκB (RANK), epidermal growth factor receptor (EGFR), STAT and focal adhesion kinase (FAK) cell signaling pathways are involved in the initiation and maintenance of the cutaneous invasion process.

The principle of management of MU is to obtain an early diagnosis and perform prompt surgical interventions. The invasion ability of MU may vary among different sites of the scalp, which may require different therapeutic strategies for surgical excision. However, no clear evidence has been provided to indicate the various invasion abilities of MU at different regions that may be used for surgical guidance. Cell adhesion molecules, the TME and cell signaling pathways are the major components that may have significant roles in burn scar carcinogenesis post burn, and also the progression of MU. In the present study, MU scalp samples were collected from the different lesion sites (core, middle and edge regions), and a comprehensive analysis was performed to detect the expression levels of invasion-associated biomarkers in those areas, including cell adhesion molecules, expression of TME-associated genes and cell signaling pathway components. Of note, the expression of biomarkers of the tumor invasiveness was different among various sites of the scalp affected by MU. Of note, high expression levels of certain biomarkers were detected in the core region of MU compared to the middle and edge areas. These results may provide information for developing appropriate therapeutic strategies of the MU treatment in the future.

Patients and methods

Patients and samples. Tissue samples, including one MU and three normal scalp samples were obtained from surgical specimens of patients at the Department of Neurosurgery, the First Affiliated Hospital of Wenzhou Medical University, China. Informed consent was obtained from all patients. For acquiring the MU tissue in different site, during the surgery, a total of nine tissue samples were obtained from three different sites of the MU tumor (3 from the core, 3 from the middle and 3 from the edge) (Fig. 1E). The other three normal scalp samples were acquired during scalp mass resection. The general information of the patient was listed in the Table I. The tissue samples were preserved immediately after excision.

Hematoxylin and eosin (H&E) staining. The patients' tissues were preserved in 10% formalin and embedded in paraffin sections. In a routine procedure, the sections were prepared and stained with H&E (12,13). A Leica DMI4000B microscope (Leica Microsystems) was used for the image capture.

mRNA isolation and reverse transcription-quantitative (RT-q)PCR. Total RNA of each sample was isolated from MU tissues and normal scalp samples by using TRIzol reagent (Tiangen Biotech Co., Ltd., Beijing, China) according to the manufacturer's instructions. RNA quantity and quality were measured using a NanoDrop ND-1000 (Thermo Fisher Scientific, Inc.). RNA samples were stored at -80˚C until further use. Approximately 2 μg of total RNA was converted to the first-strand cDNA using a SuperScript II RT system (Tiangen Biotech). qPCR was performed in a 20 μl reaction volume in the presence of SYBR® Fast qPCR Mix (Takara Biotechnology, Co., Ltd.) on an ABI Q5 Real-Time PCR (Thermo Fisher Scientific, Inc.) according to the manufacturer's protocols. The primers used are listed in Table II. The reactions were performed in triplicate and results were expressed as the ratio of the quantification cycle (Cq) value for the cDNA concentration of the target gene with normalization to GAPDH using the $2^{-\Delta\Delta Cq}$ method (14).

Western blot analysis. Firstly, the different tissue samples were lysed with RIPA lysis, which contain phosphatase inhibitors and protease inhibitor (Thermo Fisher Scientific, Inc.). After centrifuged at 12,000 rpm for 30 min, we collected the supernatant. The concentration of protein was anlyzed by Pierce bicinchoninic acid assay (BCA) protein assay kit (Thermo Fisher Scientific, Inc.). Proteins from tissue were separated in 15% SDS-PAGE and then transferred to a polyvinylidene difluoride (PVDF) filter membranes (Millipore). After blocked with 3% BSA (BioFroxx) for 2 h, the PVDF membranes were incubated at 4˚C overnight with primary antibodies against p-STAT3 (Rabbit Polyclonal, CST, #9145 1:1,000), p-EGFR (Rabbit Polyclonal, Affinity Biosciences, #AF3048, 1:1,000), p-FAK (Rabbit Polyclonal, Affinity Biosciences, #AF3398, 1:1,000) and β-actin (Rabbit Polyclonal, Abcam, ab8227, 1:1,000). PVDF membranes were washed in TBST before incubated with secondary antibody (1:5,000) for 1h at RT. The membrane were washed with PBST and then visualization by ECL HRP substrate (Advansta).

Statistical analysis. Values are expressed as the mean ± standard error of the mean. GraphPad PRISM software (version 7, GraphPad Software, Inc.) was used for the statistical data analysis. The One-way ANOVA followed by Bonferroni's Multiple Comparison was performed to determine the statistical significance of the RT-qPCR results results. $P<0.05$ was considered to indicate a statistically significant difference.

Table I. Demographic characteristics of patients.

Patient no.	Sex	Age	Localization	Histopathological type	Sample name
1	Female	41	Parietal region	Squamous cell carcinoma	MU tissue
2	Female	51	Right occipital region	Epidermoid cyst	Normal tissue
3	Male	36	Right frontal region	Liomyoma	Normal tissue
4	Female	38	Left parietal region	Root sheath cyst	Normal tissue

MU, Marjolin's ulcer.

Table II. Primer list for reverse transcription-quantitative PCR.

Gene name	Forward primer (5'-3')	Reverse primer
Periostin	ACAAGAAGAGGTCACCAAGGTC	TTGGCTTGCAACTTCCTCAC
MMP-14	GAGCATTCCAGTGACCCCTC	ACCCTGACTCACCCCCATAA
MMP-2	GGCGCGCTCACGGGT	TCAGGTATTGCACTGCCAACT
MMP-9	CGCGCTGGGCTTAGATCATT	GTTCAGGGCGAGGACCATAG
Claudin-1	CCAGTCAATGCCAGGTACGA	GGCCTTGGTGTTGGGTAAGA
Desmoglein-3	AGTGCCTCAAACTCACTGGT	ACGGACTTCCCCAGTGTTTC
E-cadherin	ATGCTGATGCCCCCAATACC	GCTGCTTGGCCTCAAAATCC
RANKL	GTACCAGGGATGTGACGTGG	TCAGGTGATCTCTCATTCTTTTCT
FAK	TCAAGCCATGGAGGCTTCAG	GGGGCTGGCTGGATTTTACT
STAT3	GAAACAGTTGGGACCCCTGA	CTCTCAATCCAAGGGGCCAG
EGFR	TATTGATCGGGAGAGCCGGA	TCGTGCCTTGGCAAACTTTC
CXCL9	TGATTGGAGTGCAAGGAACCC	AAGGGCTTGGGGCAAATTGT
GAPDH	CAGGAGGCATTGCTGATGAT	GAAGGCTGGGGCTCATTT

MMP, MMP, matrix metalloproteinase; RANKL, receptor activator of NFκB ligand; EGFR, epidermal growth factor receptor.

Results

Case report. A 41-year-old female presented with a 40-year history of scalp ulceration presented at our department. As the disease progressed, she started to experience repeated bleeding in the ulceration lesion site for about ~1 year. The patient was reported to have contracted a burn scar from fires in the parietal region of the scalp at the age of one. In the beginning, the size of the scar was close to that of a broad bean. The ulceration of the scalp gradually increased over decades and was accompanied with a mild itching and it eventually developed into a lesion with repeated bleeding one year prior to presentation. When the patient was admitted, the size of the scalp ulcers was ~8x8 cm^2 (Fig. 1A). A CT scan demonstrated the parietal bone destruction with a huge mass on top of the skull (Fig. 1C). MRI sagittal images revealed invasion of the parietal bone by the tumor tissue with the size of about ~18x9 mm^2 (Fig. 1B). A surgical operation was performed to excise the scalp ulceration and remove the affected parietal bone. The scalp ulceration was excised by leaving 1 cm of security skin margin around the scar tissue. The diseased parietal bone was resected, and the wound was reconstructed with an autologous skin flap (Fig. 1D). During the surgery, a total of nine tissue samples were obtained from three different sites of the MU tumor for further analysis (3 from the core, 3 from the middle and 3 from the edge) (Fig. 1E).

Pathological analysis of MU tissue. H&E staining was performed to pathologically analyze the MU. The MU was pathologically classified as poorly differentiated SCC (Fig. 2A) associated with skull bone invasion (Fig. 2B). After extended resection of MU lesion tissue, the residual surrounding tissue (1 cm tumor-free margin) was confirmed as the normal scalp tissue via H&E staining (Fig. 2C and D).

Distribution of invasion-associated cell adhesion molecules at different sites of MU. To validate the hypothesis that the invasive ability of tumor cells may vary among different regions of the MU, the RT-qPCR analysis was performed to detect the expression levels of the selected cell adhesion-associated molecules in different parts of the MU (core, middle, and edge sites) and the normal skin. The RT-qPCR results revealed that the expression of claudin-1, desmoglein-3 and E-cadherin in MU was significantly higher compared with that in normal scalp tissue (Fig. 3). Furthermore, the expression levels of claudin-1 and desmoglein-3 in MU (edge) were significantly increased compared with those in MU middle). However, there was no significant difference in E-cadherin expression

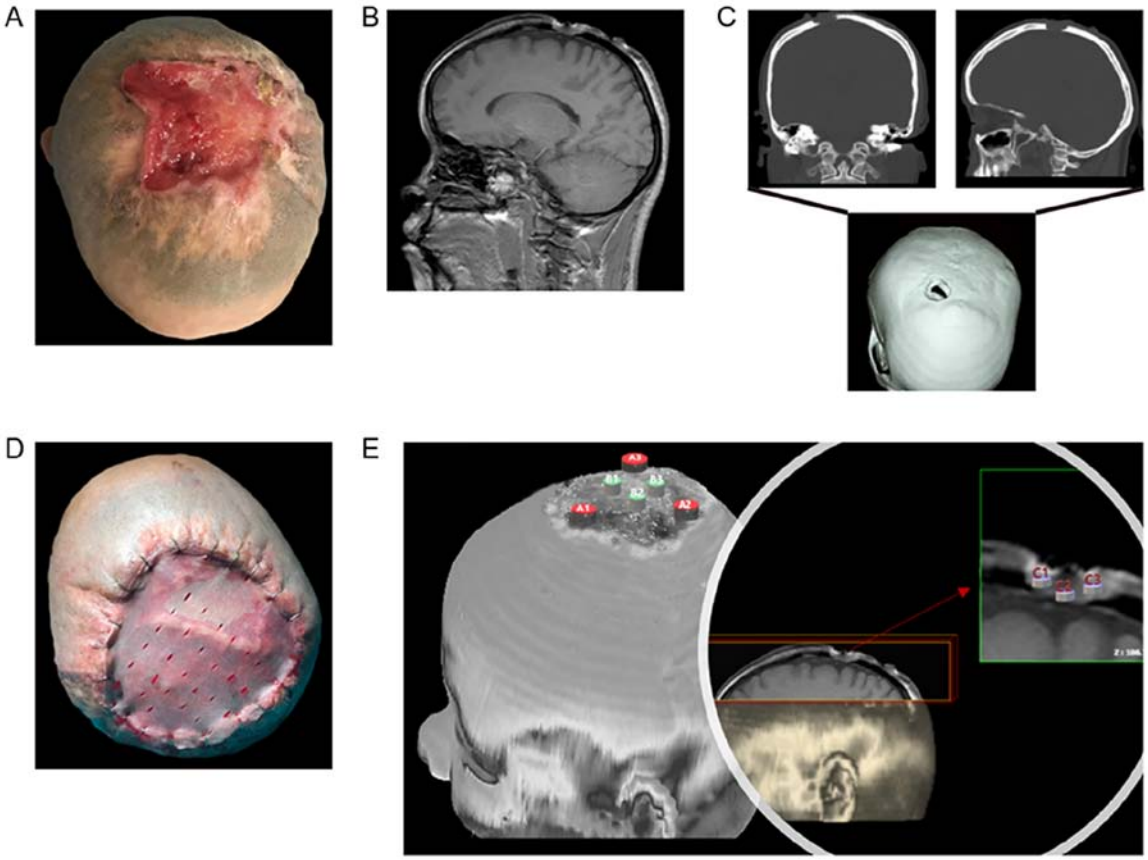

Figure 1. The patient's clinical features of MU and the illustration of tissue sample capture. (A) Image of MU, (B) MRI examination, (C) three-dimensional CT remodeling of the skull, (D) the head was covered with an autologous skin flap after MU resection, (E) illustration of tissue samples capture from different regions [3 from the core (C1-3), 3 from the middle (B1-3) and 3 from the edge (A1-3)]. MU, Marjolin's ulcer.

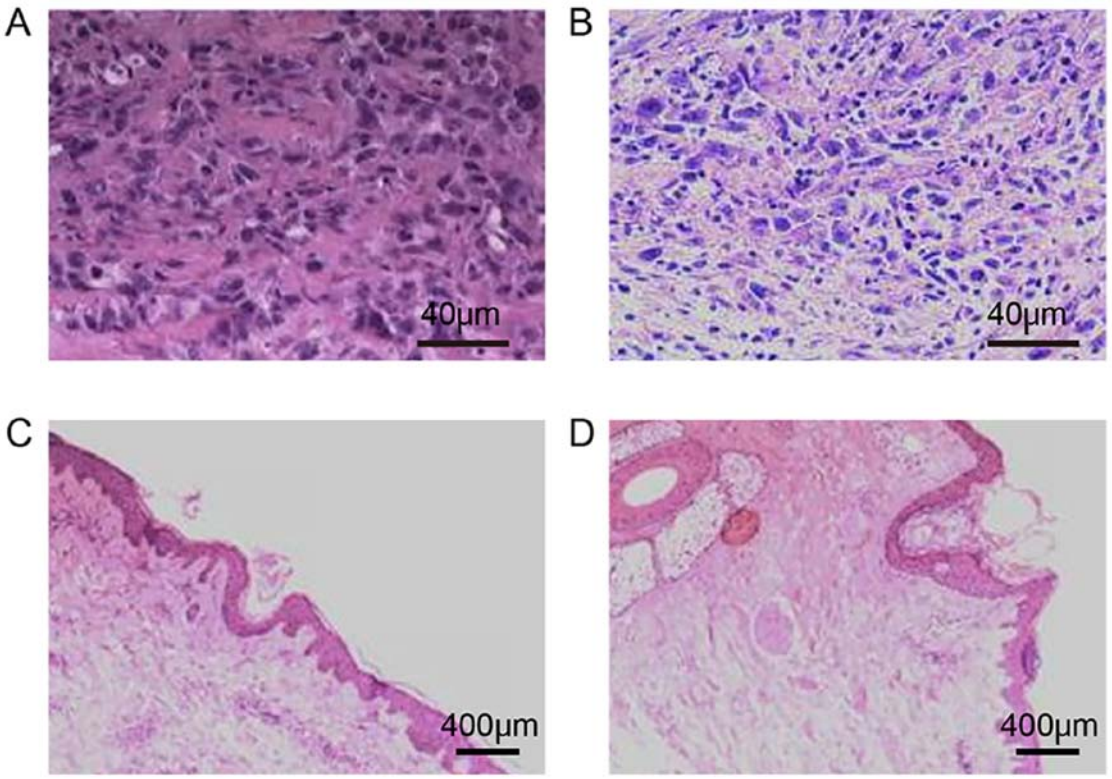

Figure 2. Pathology of MU samples. Representative images of H&E staining of (A) MU tissue, (B) skull bone tissue acquired from MU area. (C) One representative H&E staining images of surrounding healthy skin tissue after MU resection. (D) Another representative H&E staining images of surrounding healthy skin tissue. H&E, hematoxylin and eosin; MU, Marjolin's ulcer.

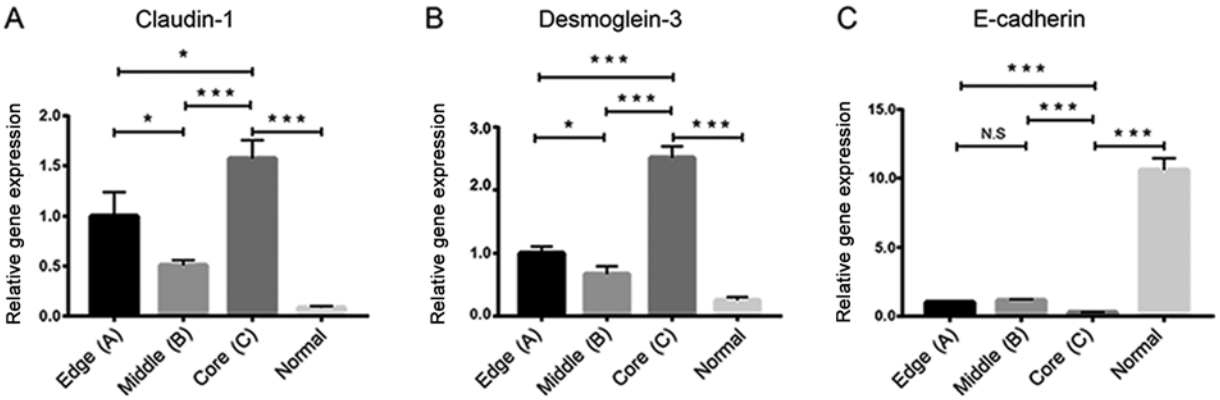

Figure 3. Expression levels of the invasion-associated cell adhesion molecules at different sites of Marjolin's ulcer. Relative mRNA expression levels of (A) claidin-1, (B) desmoglein-3 and (C) E-cadherin. Values are expressed as the standard error of the mean (n=3). *P<0.05, ***P<0.001, N.S, no significance.

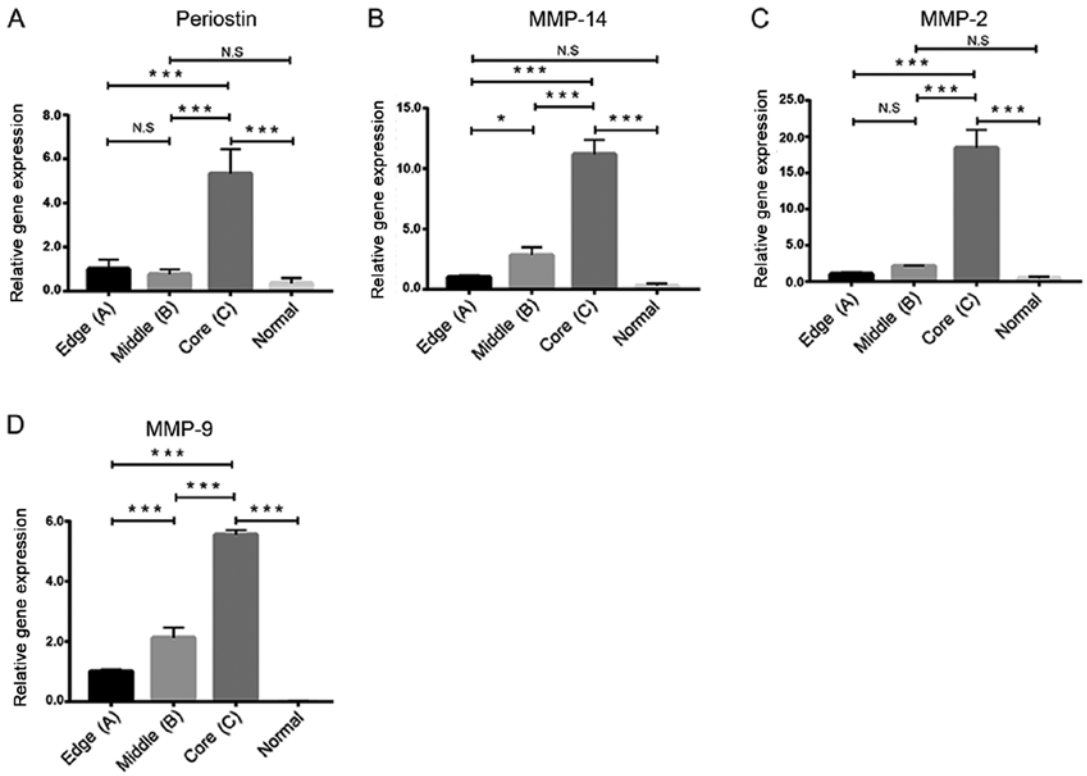

Figure 4. Expression of the invasion-associated TME molecules at different sites of Marjolin's ulcer. Relative mRNA expression levels of (A) periostin, (B) MMP-14, (C) MMP-2 and (D) MMP-9. Values are expressed as the mean ± standard error of the mean (n=3). *P<0.05, ***P<0.001, N.S., no significance; MMP, matrix metalloproteinase.

at the locations between MU (edge) and MU (middle). Of note, claudin-1 and desmoglein-3 exhibited the highest expression levels in the MU (core) samples compared with those in the samples from others parts, while E-cadherin had the lowest expression level in the core region among all samples (Fig. 3).

TME-associated gene expression at different sites of MU. According to current concepts of tumor biology, the TME is crucial for tumor cell growth. To evaluate the TME conditions at the different sites of MU, RT-qPCR analysis was performed to detect the expression levels of TME-associated biomarkers (MMP-2, MMP-9, MMP-14 and periostin). Compared with those in the normal control group, the expression of all selected TME-associated biomarkers in MU was significantly promoted. Of note, the core region of the MU lesion exhibited tissue shows the highest expression levels of MMP-2, MMP-9, MMP-14 and periostin compared to the others (Fig. 4).

Expression of tumor invasion-associated cell signaling molecules at different sites of MU. Certain cell signaling pathways are involved in the cutaneous invasion process. These representative molecular biomarkers were clearly detected by RT-qPCR experiment in the biopsy samples from the MU lesion sites, including FAK, STAT3, EGFR, C-X-C motif chemokine ligand (CXCL)9 and RANK ligand (RANKL). Of note, along with the

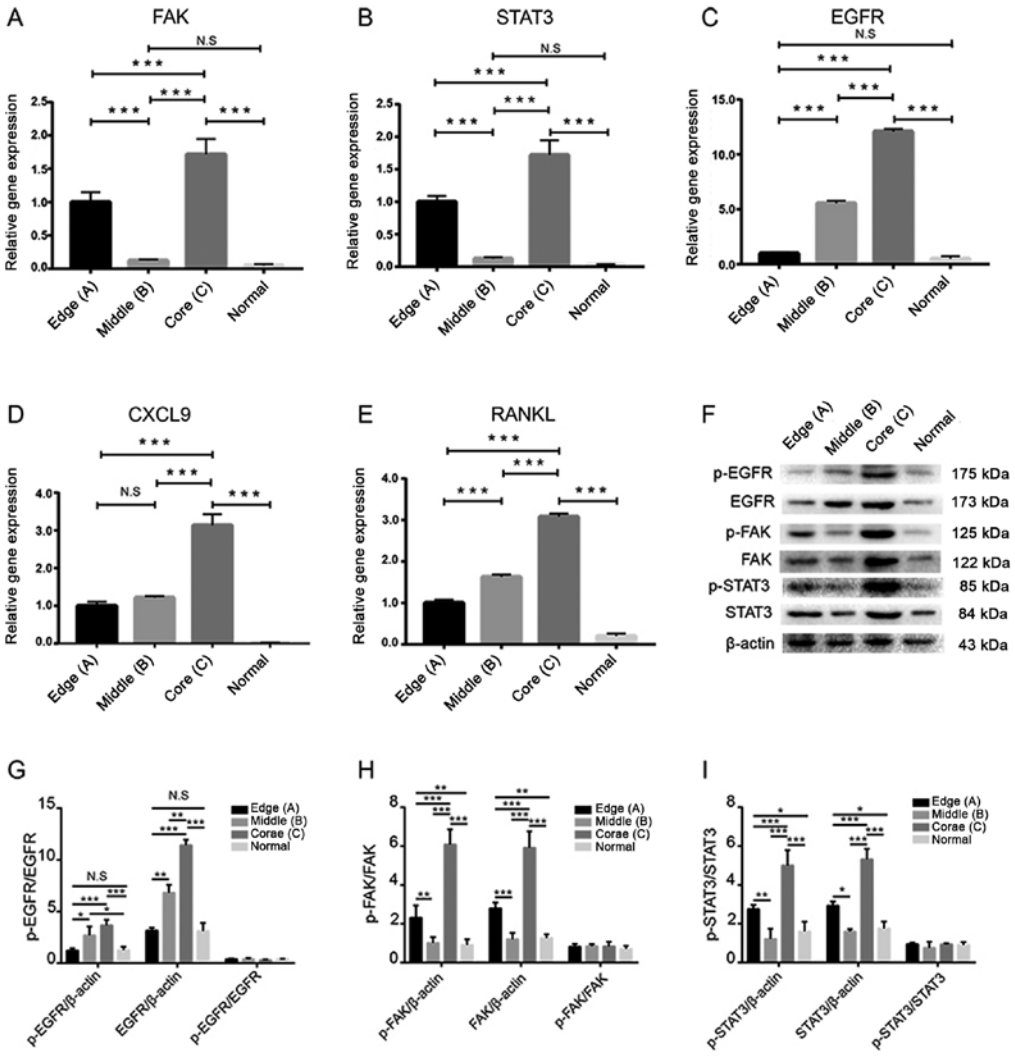

Figure 5. Expression levels of tumor invasion-associated cell signaling pathways molecules at different sites of Marjolin's ulcer. Relative mRNA expression levels of (A) FAK, (B) STAT3, (C) EGFR, (D) CXCL9 and (E) RANKL.Values are expressed as the mean ± standard error of the mean (n=3). Western blot was used to determine the protein level of phosphorylated STAT3, FAK and EGFR (F) and statistical analysis has been performed (G-I). Values are expressed as the mean ± standard error of the mean (n=3). *P<0.05, **P<0.01, ***P<0.001, N.S., no significance; FAK, focal adhesion kinase; CXCL9, C-X-C motif chemokine ligand 9; RANKL, receptor activator of NFκB ligand; EGFR, epidermal growth factor receptor; p, phosphorylated.

TME-associated molecules, all of those selected molecules were significantly overexpressed in MU (Core) samples compared to the samples from the other sites. In addition, the expression levels of all of the selected molecules in MU tissues were higher than those in the normal skin tissue (Fig. 5A-E). Furthermore, Western blot experiment has been performed to determine the level of phosphorylated STAT3, FAK and EGFR. The results also indicted that all of those phosphorylation molecules were significantly increased in MU (Core) samples compared to the samples from the other sites (Fig. 5F-I).

Discussion

MU is a rare and aggressive malignancy disease with an ominous prognosis, particularly head MU (2). Understanding the exact pathogenesis of MU may markedly enhance the effectiveness of the treatment. Due to the invasion ability of MU, the principle of wide resection of MU is critical for successful surgical treatment. In the present study, it was revealed that the various regions of a scalp MU exhibit differential invasiveness based on the expression of invasion-associated genes, which provides some insights for the surgical treatment of MU. It may be concluded that the core part of MU had invasion properties, particularly in skull invasion, which should receive sufficient attention during clinical therapy.

The acquirement of invasive properties and ability to form metastasis are a key hallmark of cancer progression. In the present, we disclosed the expression levels of several different invasion-associated biomarkers were assessed at different sites of MU, including cell adhesion-associated molecules, TME-associated molecules and certain molecules which involved in invasion-associated cell signaling pathways (8). Sinha *et al* reported that acquisition of epithelial-to-mesenchymal transition (EMT) may underlie the high metastatic rate in MU tumors (15). The abnormal expression of cell adhesion molecules is in accordance with the invasion of SCC, including claudin-1, E-cadherin and desmoglein (DSG), which represents the tumor progression ability (16). Among these, claudin-1 is well known as a key factor, which has a major role in tight junction signaling (17,18). Functional

alterations of tight junctions have been widely indicated in various types of cancers, and are closely linked related to the invasive ability of tumor cells. In addition, E-cadherin reduction is also relevant to epithelial-mesenchymal transition (EMT), which is a crucial process in cancer progression (19). Futhermore, studies have reported that desmoglein is also a molecular which highly expressed in SCC (20). In the present study, based on the analysis of the mRNA expression levels of cell adhesion molecules at different sites of MU, it was evidenced that the core site of MU had the strongest invasive properties.

In addition, several TME-associated genes (MMP-2, MMP-9, MMP-14 and periostin) also have also been selected to explore the tumor microenvironment conditions of MU (21-23). As is known, degradation of restrictive ECM proteins is regulated by matrix metalloproteinases (MMPs), which have a critical role in tumor progression regarding the invasion ability of cancer cells (24). A body of evidence has indicated that the expression of MMPs was markedly elevated in SCC (25,26). In line with this the present study also identified that the expression of MMP-2, MMP-9 and MMP-14 was obviously increased in MU tissue compared with that in the normal skin tissue. Furthermore, the core site of MU tissue exhibited the highest expression of MMPs among all of the tested samples, which indicated that the utmost ability of ECM degradation at that site. In addition, it was demonstrated that periostin as a component of the ECM, was also overexpressed in SCC (27,28). In accordance with these studies, the present results also indicate that the expression of periostin in MU's tissue is higher than that in normal tissue. The core site of the MU exhibited the highest expression levels of periostin among the different sites of the MU. In summary, the microenvironment of the core site of the MU lesion may have features of invasive tumor growth.

In addition to cell adhesion molecules and the TME, several tumor invasion-associated cell signaling molecules were also investigated in the present, including RANK/RANKL, FAK, STAT3, EGFR and CLCX9 (8). As is known, RANK/RANKL signaling is critical for osteoclastogenesis, which is an essential element that contributing to bone invasion caused by the tumor cells (29,30). The present results suggested that the expression of RANKL at the core site of MU was increased, which is in compliance with the biological function of the RANK/RANKL signaling pathway in SCC (31). Recent studies have demonstrated that FAK has multiple function in carcinogenesis, particularly in cell proliferation, cell motility, invasion, inhibition of apoptosis, angiogenesis, and immunosuppression (32-34). To discover the possible role of FAK in the present study, RT-qPCR analysis was performed, revealing that the expression level of FAK was the highest in the core region of MU tissue. Furthermore, STAT3, EGFR and CLCX9, as the essential components for invasion and metastasis, were also highly expressed in SCC (35-39). This phenomenon was also observed in the present study by demonstrating higher RNA expression level of STAT3, EGFR and CLCX9 in MU compared with that in the normal skin tissue. Except RNA expression level analysis, western blot experiment also has been used to determine the protein level of phosphorylated STAT3, FAK and EGFR. The results also indicted that all of those phosphorylation molecules were significantly increased in MU (Core) samples compared to the samples from the other sites. However, we do not have paraffin tissue section for Immunohistochemistry (IHC) analysis, which should be also important for protein expression level distribution analysis, is a main limitation in our study. Based on our results, we can conclude that the highest expression level of these biomarkers was present at the center of the MU lesion, indicating that the tumor cells in the center were more aggressive compared with those in surrounding areas.

In conclusion, the present study explored the distribution pattern of the invasion-associated biomarkers at the different sites of a head MU lesion. The results indicated that the expression levels of those invasion-associated genes at different sites of MU exhibited significant differences. The core region of MU exhibited the highest expression level, suggesting the strongest invasion ability. Of note, the present study supports that the resection of the core region and surrounding skull bone is critical for successful surgical interventions of scalp MU which may feature with skull bone invasion. The present study provides a novel and effective strategy for surgical therapy for MU. It may be proposed that the invasion-associated biomarkers at the different sites of the lesion tissue should be suggestively evaluated prior to surgery for the purpose of improving the efficacy and accuracy of MU lesion excision procedures.

Acknowledgements

Not applicable.

Funding

The present study was supported by the National Natural Science Foundation of China (grant no. 81771262), Zhejiang Health Science and Technology Project (grant no. 2016RCA022) and the Zhejiang Key Research and Development Project (grant no. 2017C03027).

Availability of data and materials

All data generated or analyzed during this study are included in the published article.

Authors' contributions

ZN, ZZ, EY, DH, CZ, KW, JY and LR designed and performed the experiments, as well as analyzed and interpreted the data. ZN, KW, JH and SY wrote and edited the manuscript. QZ, SY, JY and LR supervised the project and provided critical input. All authors gave feedback and agreed on the final version of the manuscript.

Ethics approval and consent to participate

All experiments performed in accordance with the institutional guidelines for patient's sample research and approved by the First Affiliated Hospital of Wenzhou Medical University (China).

Patient consent for publication

Not applicable.

Competing interests

The authors declare that they have no competing interests.

References

1. Yu N, Long X, Lujan-Hernandez JR, Hassan KZ, Bai M, Wang Y, Wang X and Zhao R: Marjolin's ulcer: A preventable malignancy arising from scars. World J Surg Oncol 11: 313, 2013.
2. Saaiq M and Ashraf B: Marjolin's ulcers in the post-burned lesions and scars. World J Clin Cases 2: 507-514, 2014.
3. Copcu E: Marjolin's ulcer: A preventable complication of burns? Plast Reconstr Surg 124: 156e-164e, 2009.
4. Cocchetto V, Magrin P, de Paula RA, Aidé M, Monte Razo L and Pantaleão L: Squamous cell carcinoma in chronic wound: Marjolin ulcer. Dermatol Online J 19: 7, 2013.
5. Huang CY, Feng CH, Hsiao YC, Chuang SS and Yang JY: Burn scar carcinoma. J Dermatolog Treat 21: 350-356, 2010.
6. Gül U and Kiliç A: Squamous cell carcinoma developing on burn scar. Ann Plast Surg 56: 406-408, 2006.
7. Takada H, Ibaragi S, Eguchi T, Okui T, Obata K, Masui M, Morisawa A, Takabatake K, Kawai H, Yoshioka N, *et al*: Semaphorin 4D promotes bone invasion in head and neck squamous cell carcinoma. Int J Oncol 51: 625-632, 2017.
8. Siriwardena SBSM, Tsunematsu T, Qi G, Ishimaru N and Kudo Y: Invasion-related factors as potential diagnostic and therapeutic targets in oral squamous cell carcinoma-a review. Int J Mol Sci 19: 1462, 2018.
9. Glentis A, Gurchenkov V and Matic Vignjevic D: Assembly, heterogeneity, and breaching of the basement membranes. Cell Adh Migr 8: 236-245, 2014.
10. Obayashi M, Yoshida M, Tsunematsu T, Ogawa I, Sasahira T, Kuniyasu H, Imoto I, Abiko Y, Xu D, Fukunaga S, *et al*: microRNA-203 suppresses invasion and epithelial-mesenchymal transition induction via targeting NUAK1 in head and neck cancer. Oncotarget 7: 8223-8239, 2016.
11. Witz IP: The tumor microenvironment: The making of a paradigm. Cancer Microenviron 2 (Suppl 1): 9-17, 2009.
12. Hu J, Chen L, Huang X, Wu K, Ding S, Wang W, Wang B, Smith C, Ren C, Ni H, *et al*: Calpain inhibitor MDL28170 improves the transplantation-mediated therapeutic effect of bone marrow-derived mesenchymal stem cells following traumatic brain injury. Stem Cell Res Ther 10: 96, 2019.
13. Ni H, Yang S, Siaw-Debrah F, Hu J, Wu K, He Z, Yang J, Pan S, Lin X, Ye H, *et al*: Exosomes derived from bone mesenchymal stem cells ameliorate early inflammatory responses following traumatic brain injury. Front Neurosci 13: 14, 2019.
14. Ding S, Zhuge W, Hu J, Yang J, Wang X, Wen F, Wang C and Zhuge Q: Baicalin reverses the impairment of synaptogenesis induced by dopamine burden via the stimulation of $GABA_AR$-TrkB interaction in minimal hepatic encephalopathy. Psychopharmacology (Berl) 235: 1163-1178, 2018.
15. Sinha S, Su S, Workentine M, Agabalyan N, Cheng M, Gabriel V and Biernaskie J: Transcriptional analysis reveals evidence of chronically impeded ECM turnover and epithelium-to-mesenchyme transition in scar tissue giving rise to Marjolin's ulcer. J Burn Care Res 38: e14-e22, 2017.
16. Sherrill JD, Kc K, Wu D, Djukic Z, Caldwell JM, Stucke EM, Kemme KA, Costello MS, Mingler MK, Blanchard C, *et al*: Desmoglein-1 regulates esophageal epithelial barrier function and immune responses in eosinophilic esophagitis. Mucosal Immunol 7: 718-29, 2014.
17. Dos Reis PP, Bharadwaj RR, Machado J, Macmillan C, Pintilie M, Sukhai MA, Perez-Ordonez B, Gullane P, Irish J and Kamel-Reid S: Claudin 1 overexpression increases invasion and is associated with aggressive histological features in oral squamous cell carcinoma. Cancer 113: 3169-3180, 2008.
18. Oku N, Sasabe E, Ueta E, Yamamoto T and Osaki T: Tight junction protein claudin-1 enhances the invasive activity of oral squamous cell carcinoma cells by promoting cleavage of laminin-5 gamma2 chain via matrix metalloproteinase (MMP)-2 and membrane-type MMP-1. Cancer Res 66: 5251-5257, 2006.
19. Tunggal JA, Helfrich I, Schmitz A, Schwarz H, Günzel D, Fromm M, Kemler R, Krieg T and Niessen CM: E-cadherin is essential for in vivo epidermal barrier function by regulating tight junctions. EMBO J 24: 1146-1156, 2005.
20. Huang CC, Lee TJ, Chang PH, Lee YS, Chuang CC, Jhang YJ, Chen YW, Chen CW and Tsai CN: Desmoglein 3 is overexpressed in inverted papilloma and squamous cell carcinoma of sinonasal cavity. Laryngoscope 120: 26-29, 2010.
21. de Vicente JC, Lequerica-Fernández P, Santamaría J and Fresno MF: Expression of MMP-7 and MT1-MMP in oral squamous cell carcinoma as predictive indicator for tumor invasion and prognosis. J Oral Pathol Med 36: 415-424, 2007.
22. Bodnar M, Szylberg L, Kazmierczak W and Marszalek A: Differentiated expression of membrane type metalloproteinases (MMP-14, MMP-15) and pro-MMP2 in laryngeal squamous cell carcinoma. A novel mechanism. J Oral Pathol Med 42: 267-274, 2013.
23. Kwon YJ, Lee SJ, Koh JS, Kim SH, Kim YJ and Park JH: Expression patterns of aurora kinase B, heat shock protein 47, and periostin in esophageal squamous cell carcinoma. Oncol Res 18: 141-151, 2009.
24. Reddy KB, Nabha SM and Atanaskova N: Role of MAP kinase in tumor progression and invasion. Cancer Metastasis Rev 22: 395-403, 2003.
25. Samantaray S, Sharma R, Chattopadhyaya TK, Gupta SD and Ralhan R: Increased expression of MMP-2 and MMP-9 in esophageal squamous cell carcinoma. J Cancer Res Clin Oncol 130: 37-44, 2004.
26. Yokoyama K, Kamata N, Fujimoto R, Tsutsumi S, Tomonari M, Taki M, Hosokawa H and Nagayama M: Increased invasion and matrix metalloproteinase-2 expression by Snail-induced mesenchymal transition in squamous cell carcinomas. Int J Oncol 22: 891-898, 2003.
27. Ibbetson SJ, Pyne NT, Pollard AN, Olson MF and Samuel MS: Mechanotransduction pathways promoting tumor progression are activated in invasive human squamous cell carcinoma. Am J Pathol 183: 930-937, 2013.
28. Kashyap MK, Marimuthu A, Peri S, Kumar GS, Jacob HK, Prasad TS, Mahmood R, Kumar KV, Kumar MV, Meltzer SJ, *et al*: Overexpression of periostin and lumican in esophageal squamous cell carcinoma. Cancers (Basel) 2: 133-142, 2010.
29. Jimi E, Shin M, Furuta H, Tada Y and Kusukawa J: The RANKL/RANK system as a therapeutic target for bone invasion by oral squamous cell carcinoma (Review). Int J Oncol 42: 803-809, 2013.
30. Kitazawa S and Kitazawa R: RANK ligand is a prerequisite for cancer-associated osteolytic lesions. J Pathol 198: 228-236, 2002.
31. Chuang FH, Hsue SS, Wu CW and Chen YK: Immunohistochemical expression of RANKL, RANK, and OPG in human oral squamous cell carcinoma. J Oral Pathol Med 38: 753-758, 2009.
32. Murata T, Naomoto Y, Yamatsuji T, Okawa T, Shirakawa Y, Gunduz M, Nobuhisa T, Takaoka M, Sirmali M, Nakajima M, *et al*: Localization of FAK is related with colorectal carcinogenesis. Int J Oncol 32: 791-796, 2008.
33. Schober M and Fuchs E: Tumor-initiating stem cells of squamous cell carcinomas and their control by TGF-β and integrin/focal adhesion kinase (FAK) signaling. Proc Natl Acad Sci USA 108: 10544-10549, 2011.
34. Miyazaki T, Kato H, Nakajima M, Sohda M, Fukai Y, Masuda N, Manda R, Fukuchi M, Tsukada K and Kuwano H: FAK overexpression is correlated with tumour invasiveness and lymph node metastasis in oesophageal squamous cell carcinoma. Br J Cancer 89: 140-145, 2003.
35. Grandis JR, Drenning SD, Zeng Q, Watkins SC, Melhem MF, Endo S, Johnson DE, Huang L, He Y and Kim JD: Constitutive activation of Stat3 signaling abrogates apoptosis in squamous cell carcinogenesis in vivo. Proc Natl Acad Sci USA 97: 4227-4232, 2000.
36. Kijima T, Niwa H, Steinman RA, Drenning SD, Gooding WE, Wentzel AL, Xi S and Grandis JR: STAT3 activation abrogates growth factor dependence and contributes to head and neck squamous cell carcinoma tumor growth in vivo. Cell Growth Differ 13: 355-362, 2002.
37. Rubin Grandis J, Melhem MF, Gooding WE, Day R, Holst VA, Wagener MM, Drenning SD and Tweardy DJ: Levels of TGF-alpha and EGFR protein in head and neck squamous cell carcinoma and patient survival. J Natl Cancer Inst 90: 824-832, 1998.
38. Hanawa M, Suzuki S, Dobashi Y, Yamane T, Kono K, Enomoto N and Ooi A: EGFR protein overexpression and gene amplification in squamous cell carcinomas of the esophagus. Int J Cancer 118: 1173-1180, 2006.
39. Li Z, Liu J, Li L, Shao S, Wu J, Bian L and He Y: Epithelial mesenchymal transition induced by the CXCL9/CXCR3 axis through AKT activation promotes invasion and metastasis in tongue squamous cell carcinoma. Oncol Rep 39: 1356-1368, 2018.